TIMING AND PARAGENESIS OF THE CALCITE FRACTURE FILL IN THE WOODFORD SHALE

By

JACQUEINE RENE BERRYMAN

Bachelor of Arts/Science in Geology

Oklahoma State University

Stillwater, OK

December, 2006

Submitted to the Faculty of the
Graduate College of the
Oklahoma State University
in partial fulfillment of
the requirements for
the Degree of
MASTER OF SCIENCE
July 2012

TIMING AND PARAGENESIS OF THE CALCITE FRACTURE FILL IN THE WOODFORD SHALE

Thesis Approved:

Dr. Jay Mason Gregg

Thesis Adviser

Dr. James Owen Puckette

Dr. Darwin Boardman

Dr. Sheryl A. Tucker

Dean of the Graduate College

TABLE OF CONTENTS

Chapter Page

LIST OF TABLES

LIST OF FIGURES

CHAPTER I

INTRODUCTION

In core of the Woodford shale from the Arkoma Basin, fracture fill calcite is found at different depths. One of the chief characteristics of the Woodford shale is that it is brittle; due to the silica-rich mineralogy (Brown, 2008). This brittleness allows for an abundance of natural fractures. Understanding the timing of the fracturing of the shale and the timing of the calcite fill is important to understanding the basin evolution of the Arkoma Basin.

Previously electron microprobe research on the fracture fill of the Woodford Shale in the Poe 1-29 core was conducted by Berryman et al. (2007). The results of this study found that the lower portion of the Woodford Shale contains fracture filling calcite and pyrite. The middle portion of the Woodford contains calcite and dolomite cement, while pyrite in the fracture fill was rare. The upper portion contains calcite fracture fill with pyrite occurring in the shale matrix (Berryman et al., 2007).

This study is potentially important to the oil and gas industry as it provides information that could lead to the prediction of where fracture filling calcite cement in the Woodford shale might occur and what kind of fluids formed the cement. The study also provides a paragenetic sequence for the calcite relative to other diagenetic events. The main goals of this study are: A) to define the physical characteristics of the precipitating fluids, B) to understand the origin of both the aqueous and hydrocarbon fluids and C) to determine the timing of the fracturing of the Woodford shale and the timing of fluid migration. We hypothesize that the calcite fracture fill was formed at high temperatures from basinal fluids soon after the natural fracturing of the Woodford Shale and the uplift of the Arkoma foreland basin during the Pennsylvanian-Permian Ouachita orogeny.

CHAPTER II

REGIONAL GEOLOGY

Arkoma Basin Evolution

The Arkoma Basin is an arcuate foreland basin north of the Ouachita fold and thrust belt (Cemen et al., 1996; Sutherland, 1988) (Fig. 1). During the time of the Woodford sediment deposition, the area of the present day Arkoma Basin was part of a broad, stable shelf along a passive continental margin. During the Middle Mississippian (Chesterian) through the Middle Pennsylvanian (early Atokan) there was varying depositional patterns on the shelf due to the development of carbonates and the influx of terrigeneous clastics from the north (Sutherland, 1988). During the middle Atokan a flexural down-warping of the southern margin of the shelf and down-to-the-south normal faults developed sequentially to the north because of the collapse of the Ouachita trough (Sutherland, 1988). Through the late Atokan the axis of deposition shifted northward with the development of a fully formed and subsiding foreland basin. Recurrent uplift of the Ouachita fold belt coincided with the disruption of the Arkoma Basin which experienced compression and folding and ended the progressive down-warping of the southern shelf and shifted the depocenter to the northwest (Sutherland, 1988; Elmore et al., 1990).

Woodford Shale

The Woodford Shale and equivalent units are widely distributed in North America and, where they are thermally mature are likely hydrocarbon source rocks (Lambert 1994; Comer, 2005). The Woodford's thermal maturity, geological setting, lithology, mineralogy and amount and type of total organic carbon make it an important gas play in the state of Oklahoma (Brown, 2008).

Amsden and Klapper (1972) used conodont biostratigraphy to date the basal Woodford to Middle-Late Devonian, Givetian to early Famennian in age. Hass and Huddle (1965) and Over and Barrick (1990) dated the upper Woodford to be largely Late Devonian, Famennian; extending unconformably upward into the lower Mississippian (Lambert 1994). In the Arkoma Basin, the Woodford Shale is unconformably overlain by the Mississippian age Caney Shale and is unconformably deposited either on the Silurian-Devonian Hunton Group or the Ordovician Sylvan Shale (Figure 2).

During the Late Devonian, the southern midcontinent was positioned along the western margin of North America in the warm dry tropics near 15° south latitude (Comer, 1991) (Figure 3). Formation of the Woodford began in the deepest parts of the Delaware, Val Verde, Anadarko, and Arkoma basins as they were flooded by rising sea levels. The newly formed sea, which extended inland from the continental margin, had irregular bottom topography and scattered land masses (Comer, 2005).

Woodford Geochemical Characteristics

The regional distribution of the total organic carbon and organic matter type of the Woodford Shale is explained as a response to the Late Devonian paleogeography

(Comer, 1992b). The organic content of the Woodford Shale in Oklahoma is dominated by a northwest-southeast trend of high total organic carbon (TOC) located in the center of Oklahoma. Comer‘s (1992b) data suggest that TOC increases toward the Arkoma Basin. The lowest TOC values are found in the core area of the Ouachita tectonic belt (Comer, 1992b).

The Woodford Shale reaches its highest thermal maturity in the Anadarko, Delaware, and Arkoma basins where it is most deeply buried and contains predominantly oil-prone type II kerogen (Comer and Hench, 1987; Comer, 2005). In the deep basins, the Woodford Shale is in the oil generation window (Comer, 1991, 1992). The Woodford is less mature on the structural highs (Comer, 2005). The exclusive occurrence of gas in the deep basins is due to high thermal maturity. Cardott (2001) based this conclusion on the occurrence of bituminous-rank coal beds at the surface, however, the presence of pyrobitumen in the post-mature Woodford Shale points towards oil generative organic matter being present originally. The greatest gas potential is 600 x 10^{12} ft^3 in an area that includes the deepest part of the Anadarko and Arkoma basins (Comer, 2005).

Hydrocarbon Migration in the Arkoma Basin

Comer (1992b) studied the petroleum generation and oil expulsion history of the Upper Devonian source beds, which included the Woodford Shale. In central and southern Oklahoma, the Woodford is at an early stage of petroleum generation. Comer (1992b) found that although some of the oil migrated from mature sections buried deeper in adjacent basins, most of the oil was expelled from local source beds at an early oil-generation stage.

Comer and Hinch (1987) imply that the timing of oil expulsion may vary depending upon the amount and type of organic matter in the source rock. The Woodford is a very rich, oil-prone source rock and may yield a large enough volume of oil to saturate the pore space of the rock, even at the very early stages of oil generation. Therefore, expulsion likely began at an early time and continued as long as oil was generated and internal pressure was maintained. This occurred regardless of the specific thermal maturity or whether the main stage of oil generation has been reached (Comer and Hinch, 1987).

Cander et al., (2007) conducted a detailed basin modeling, petroleum migration, and pore pressure study of the Arkoma Basin. This study found that oil and gas generated by the Woodford Shale migrated laterally in the pre-Atokan rocks during the late Pennsylvanian time through sandstone and carbonate beds. Vertical migration was stopped by a pressure seal located near the base of the Atoka-age synorogenic, foreland sediments. With continued burial, the oil that was not flushed from the system was cracked into gas. Later uplift caused the supra-Spiro pressure seal to breach and volumes of gas were able to migrate vertically into the foreland sediments (Cander et al, 2007).

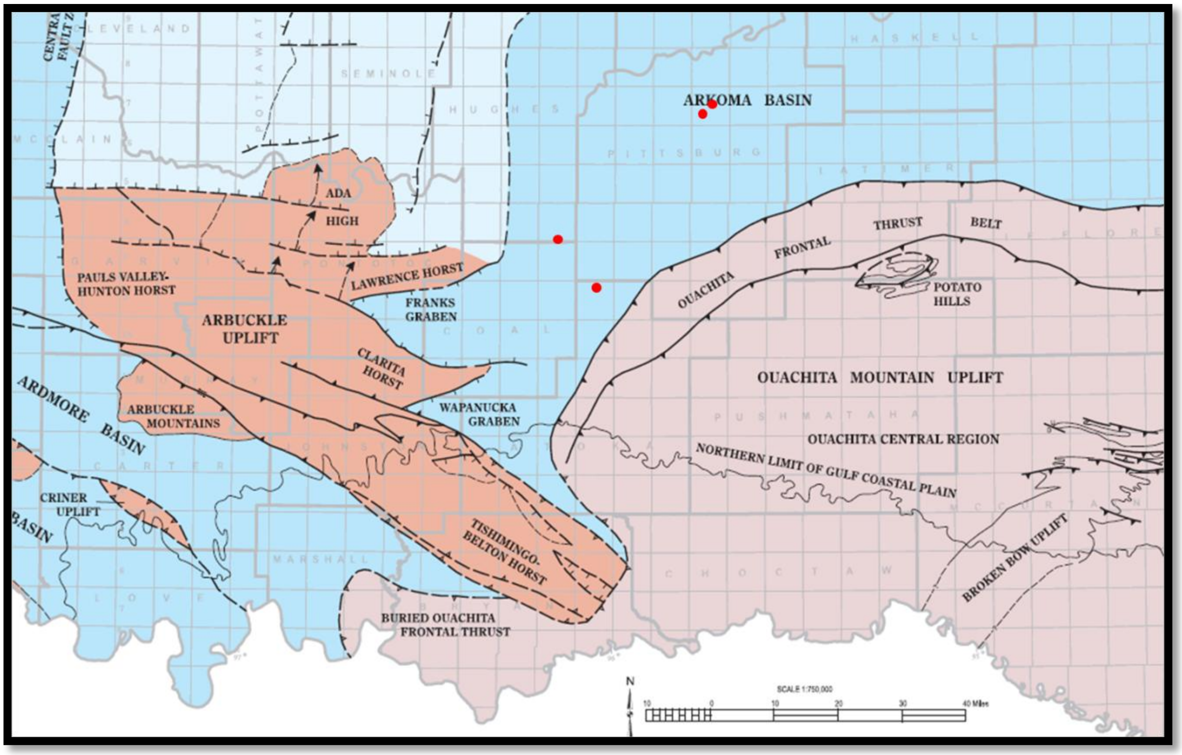

Fig. 1. Regional map showing the location of cores used in this study (red circles) in the Arkoma Basin of south eastern Oklahoma. The blue color represents the deep basin, the light blue represents the shelves and the shallow basins, the lavender color represents the detachment uplift, and the pink represents basement-rooted uplifts. Scale bar = 40 miles or 64.4 km. Map from the Oklahoma Geological Survey and compiled by R.A. Northcutt and J.A. Campbell, 1995.

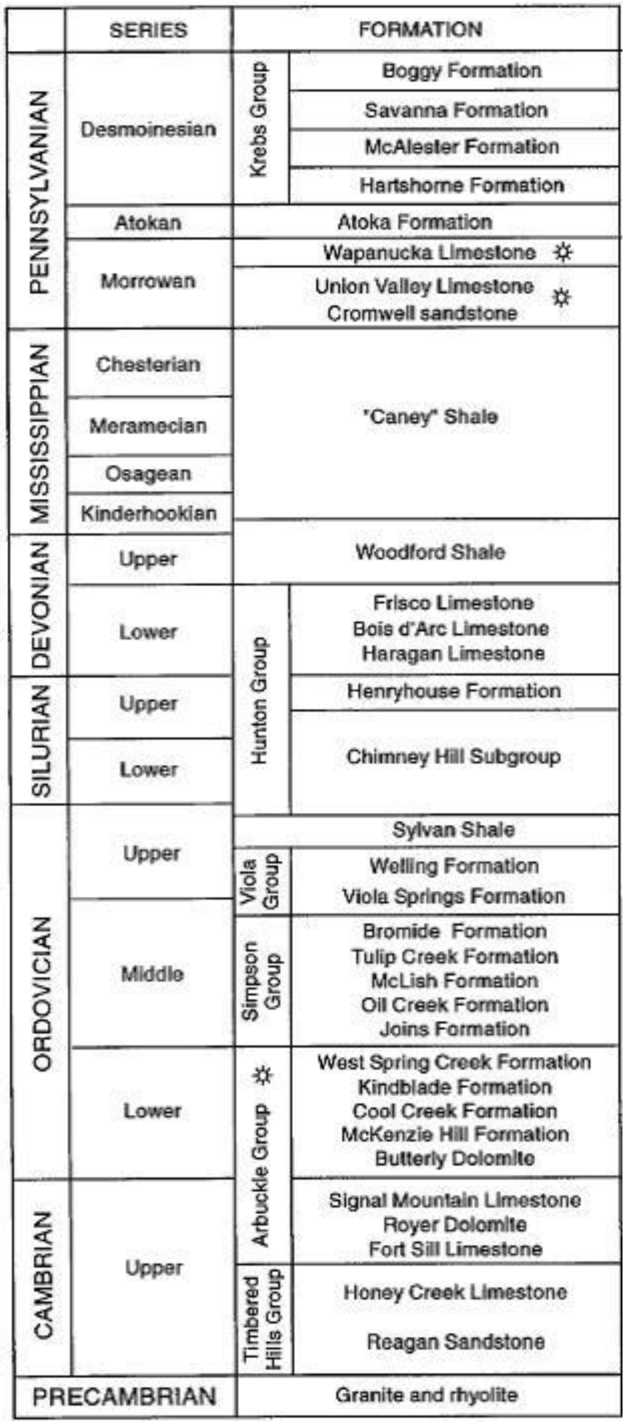

	SERIES	FORMATION	
PENNSYLVANIAN	Desmoinesian	Krebs Group	Boggy Formation
			Savanna Formation
			McAlester Formation
			Hartshorne Formation
	Atokan	Atoka Formation	
	Morrowan	Wapanucka Limestone ☼	
		Union Valley Limestone Cromwell sandstone ☼	
MISSISSIPPIAN	Chesterian	"Caney" Shale	
	Meramecian		
	Osagean		
	Kinderhookian		
DEVONIAN	Upper	Woodford Shale	
	Lower	Hunton Group	Frisco Limestone Bois d'Arc Limestone Haragan Limestone
SILURIAN	Upper		Henryhouse Formation
	Lower		Chimney Hill Subgroup
ORDOVICIAN	Upper	Sylvan Shale	
		Viola Group	Welling Formation Viola Springs Formation
	Middle	Simpson Group	Bromide Formation Tulip Creek Formation McLish Formation Oil Creek Formation Joins Formation
	Lower	Arbuckle Group ☼	West Spring Creek Formation Kindblade Formation Cool Creek Formation McKenzie Hill Formation Butterly Dolomite
CAMBRIAN	Upper		Signal Mountain Limestone Royer Dolomite Fort Sill Limestone
		Timbered Hills Group	Honey Creek Limestone Reagan Sandstone
PRECAMBRIAN		Granite and rhyolite	

Fig. 2. Stratigraphic nomenclature for the Arkoma Basin (from Hemish and Suneson, 1997, fig. 2). The Hunton Group rocks are missing in the cores from Pittsburg County where the Woodford sediment was deposited directly on the Sylvan Shale.

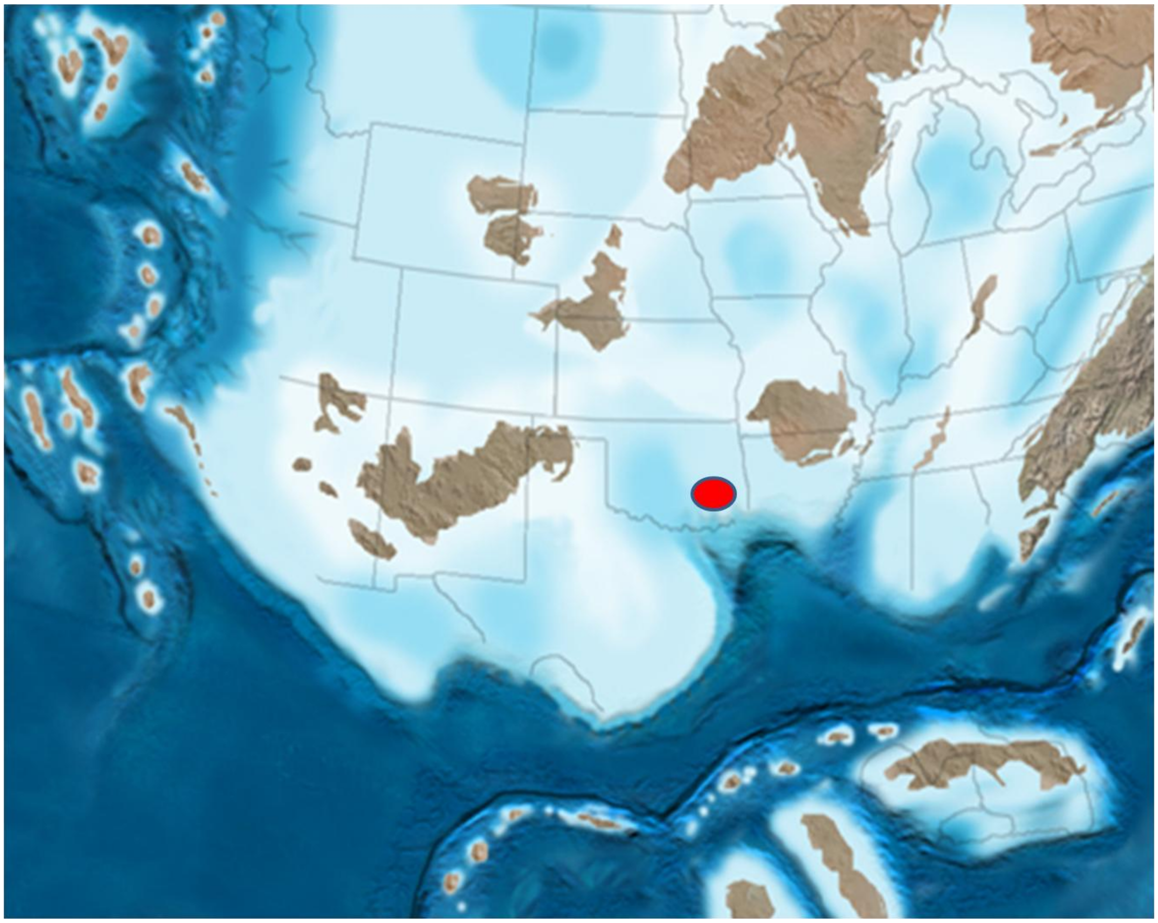

Fig. 3. The paleogeography of North America during the Late Devonian, during the deposition of the Woodford sediments (From Blakey, NAU Geology, 2012). The red circle represents the approximate location of the Arkoma Basin.

CHAPTER III

METHODS

Cores were acquired from Newfield Exploration and PetroQuest Energy, Inc. from petroleum wells in the Arkoma Basin. A detailed description of each core was made (see plates 1-3) and fractures were identified as horizontal or vertical, open or cemented. Any core found to have fracture cement was sampled at those intervals. A basic petrographic analysis was carried out to note the prominent constituents, shale matrix, fossil assemblages and type of pore space. Thin-sections (standard) and doubly polished fluid inclusion plates (60-100 microns thick) of the fracture fill from both cores were made by High Mesa Petrographics.

Fluid inclusion microthermometric measurements were conducted with a Linkam THMSG 600 heating and cooling stage mounted on an Olympus BX51 Epi-Fluorescence Microscope equipped with a Q Color 3 camera, and using Linkam CI 94 computer interface and Linksys 32 software. Temperatures of homogenization (T_h) and ice melt (T_m) have errors of ± 1º C based on reproducibility of the data. All inclusions measured were two phase primary and secondary inclusions as defined by Reynolds and Goldstein (1994). The inclusions contained no daughter minerals and had a size range of 1-4µm. Salinities were calculated from T_m measurements using Bodnar's (1992) equations. Cathodoluminescence (CL) analysis was used for the delineation of compositional zoning within the calcite fill (Frank et al., 1982). The CL petrography of the calcite fill was conducted using a CITL CL8200 MK5-1 Optical Cathodoluminescence system. Photomicrographs will be obtained on an Olympus BX51 petrographic microscope with Q Imaging Micropublisher 5.0 RTV cooled camera.

Stable carbon and oxygen isotope analysis of the calcite fracture fill was performed at the Boone Pickens School of Geology Isotope Geochemistry Lab. Carbon has two stable isotopes ^{12}C and^{13}C, carbon isotope ratios are measured against Vienna Pee Dee Belemnite (VPDB).

CHAPTER IV

Results

Core Description

The drill core acquired for this research came from three counties in the Arkoma Basin. The Mr. Bill 1-30 core and the Jerry Steidley 5-16 CW core came from Pittsburg County, OK. The Poe 1-29 core came from Hughes County, OK and the 1-H-12 Newberry well came from Atoka County, OK (Fig. 4). Core descriptions (Plates 1, 2 and 3) were made of each core except the Newberry 1-H-12 because only core samples were obtained. Both the Pittsburg County cores lacked fracture fill cement. The fractures were largely open horizontal fractures. The calcite fracture fills sampled in this study were taken from various depths of the Poe 1-29 core and from the core samples of the Newberry 1-H-12 core.

Petrography

Examples of the shale fractures and fill in the Poe 1-29 core are shown in Figure 5. Both the Poe 1-29 and the 1-H-12 Newberry cores have very similar composition; a black siliceous, fossiliferous (micro-fossils), organic rich shale. Pyrite is common and occurs in lenses which can be seen in hand samples. The majority of microfossils are Spumellarian Radiolarians; which are radially- symmetrical forms and are common constituents of pelagic deposits throughout the Phanerozoic (Fig. 6A, 6B and 6C). Sponge spicules and shell fragments were also observed (Fig. 6D and 6E).

Cathodoluminescence

Using cathodoluminescence (CL) imaging, the fractures of the Poe 1-29 and the Newberry 1-H-12 were observed to contain calcites with varying CL zoning patterns.

Poe 1-29 Core

Fractures in the Poe 1-29 core at a depth of 2360.4 m display three generations of calcite cement; 1) CL equant sparry calcite cement; 2) a moderately CL microspar; 3) a dully CL microspar (Fig. 7A and 7B) This microstratigraphy is observed throughout the fractures at this depth.

At depth 2360.7 m the Poe core contains a brecciated zone in the shale matrix. The cement is a dully luminescent fibrous calcite with a brightly CL zoned rim. Smaller fractures are filled with a dully luminescent sparry calcite (Fig. 7C and 7D).

At depth 2362.5 m shale fractures contain a sparry calcite that transitions to a dully CL microspar in the center of the fracture. Other fractures show one generation of calcite precipitation of a CL sparry calcite. The shale matrix has a moderately luminescent microspar that precipitated in the shale pore space (Fig. 7E and 7F).

At depth 2389.0 m the shale fractures display two generations of calcite precipitation; a non-CL blocky calcite and a bright CL microspar in the pore space of the surrounding shale matrix (Fig. 7G and 7H). The same CL microstratigraphy is observed in other fractures at this depth.

1-H-12 Newberry Core

Samples obtained from the 1-H-12 Newberry core a depth of 3995.3 m exhibit a CL microstratigraphy consisting of moderately CL microspar and sparry calcite with a dully CL microspar (Fig. 8A and 8B). Larger fractures, at this same depth, exhibit a relatively thick zone of dully CL sparry calcite cement and a thin yellowish, moderately CL zone of sparry calcite cement (Fig. 8C and 8D). At a depth of 3996.0 m the fractures display three generations of calcite precipitation; 1) an orange CL zone of microspar within the pore space of the shale matrix and along the fracture wall; 2) a yellowish moderately CL zone of microspar; and 3) a dully CL zone of sparry calcite cement (Fig. 8E and 8F). The same CL microstratigraphy is observed throughout fractures at this depth.

Stable Isotope Analysis

The calcite fracture fill in the Poe 1-29 core displays δ^{13}C values (Table 1, Appendix) that range from -4.438 to -23.026‰ VPDB (Fig. 9) and δ^{18}O values ranging from -1.053 to -7.406‰ VPDB respectively. The average δ^{18}O value is -4.453 ‰ VPBD. The average δ^{13}C value is -12.549‰ VPDB- The highest δ^{13}C values are from a depth of 2376.2 m and the lowest from 2360.4 m. The highest δ^{18}O values are from a depth of 2360.4 m. and the lowest from 2376.2 m.

The calcite fracture fill in the Newberry 1-H-12 core show $\delta^{13}C$ values that range from -8.691 to -9.178‰ VPDB (Fig. 9) and $\delta^{18}O$ values that range from -3.071 to -3.464‰ VPDB respectively. The average $\delta^{18}O$ value is -3.475‰ VPDB. The average $\delta^{13}C$ value is -8.971‰ VPDB. The highest $\delta^{13}C$ values are from a depth of 3995.3 m and the lowest from 3995.6 m. The highest $\delta^{18}O$ values are from a depth of 3995.3 m. and the lowest from 3995.6 m.

The calculated $\delta^{18}O_{water}$ values for the formation waters in the Poe 1-29 ranged from 25.84‰ to 26.15‰ VSMOW, with an average of 25.96‰ VSMOW with a difference of $\delta^{18}O_{calcite}$ to $\delta^{18}O_{water}$ of 0.44‰. The values for the Newberry 1-H-12 had $\delta^{18}O_{water}$ values ranging from 26.35‰ to 27.27‰ VSMOW, with the difference from $\delta^{18}O_{calcite}$ to $\delta^{18}O_{water}$ of 0.46‰.

Fluid Inclusion Analysis

Measured two-phase fluid inclusions in the calcite fracture fill range in size from 1-4 μm and the calcite crystals containing these inclusions were formed in fractures that range from 10 microns to 2.7 mm in width. Two phase aqueous fluid inclusions are rare in the fracture fill and difficult to measure due to the small size of the inclusions. Four primary fluid inclusions and one secondary inclusion was measured in the Poe 1-29 core and two primary fluid inclusion assemblages and one secondary fluid inclusion assemblage was measured in the Newberry 1-H-12 core. The aqueous fluid inclusions in the Poe 1-29 and the Newberry 1-H-12 samples had similar average homogenization temperatures (T_h) (Fig. 10), 100°C and 95°C respectively. The Poe 1-29 inclusions had calculated salinities that ranged from 0.18 to 7.17 wt% Sodium Chloride (NaCl); while the Newberry 1-H-12 inclusions had salinities that ranged from 2.57 to 12.05 wt% NaCl. None of the measured two phase fluid inclusions exhibit excitation under fluorescence.

Measured fluid inclusions in the Poe 1-29 (Fig. 11) have homogenization temperatures (T_h) ranging from 80-113°C (Table 2, Appendix). The average of the final melting temperatures (T_m) was -2.5°C; while the average salinity value was 4.07 wt% NaCl. All temperature measured values are for single fluid inclusions.

Measured inclusions in the Newberry 1-H-12 (Fig. 12) have T_h values ranging from 81.8 to 110°C. The average temperature values for T_m was +4.62°C; while the average salinity value was 6.47 wt% NaCl. Three of the four homogenization temperatures reported for the Newberry 1-H-12 core are from fluid inclusion assemblages (Table 1): 1) depth 3995.3, an assemblage of 3 inclusions along a growth boundary (Fig. 12 A), 2) depth 3995.6 m, an assemblage of 3 inclusions within a single calcite crystal (Fig. 12 B), and 3) depth 3995.9 m, an assemblage of 2 inclusions along a growth boundary (Fig. 12 D).

The Newberry and Poe core samples both contain one-phase petroleum inclusions that appear clear in plain polarized light (PPL) but fluoresce when viewed with epi-fluorescence (Fig. 13 & 14). The large majority of the petroleum inclusions are irregularly shaped, primary, petroleum filled inclusions that range from 4 to 9µm and fluoresced greenish yellow allowing an approximation of an API gravity of 30-35° (Goldstein & Reynolds, 1994). One imaged primary petroleum inclusion fluoresced bluish green indicating an API of 35-40° (Fig. 14E). A mean API gravity for the Woodford Shale in Oklahoma was calculated using 77 Woodford oils and was found to be 39 ± 9.3 ° (Comer and Hinch, 1987).

Paragenesis

Paragenetic sequences for the Poe 1-29 and the Newberry 1-H-12 were created using the petrographic observations above (Fig. 15A and 15B). Petrographic analysis and the presence of petroleum inclusions indicate that soon after the fracturing of the Woodford shale, hydrocarbon generation and migration had begun. Brightly CL microspar initially precipitated in the fractures and in the pore space of the shale matrix, followed by brightly CL sparry calcite precipitation, suggesting a fluid with low Fe/Mn. CL intensity displayed by calcite is controlled by the Fe/Mn ratio of a given calcite zone, not by the absolute concentrations of either cation (Frank et al., 1982). This was followed by precipitation of a non-CL (Poe 1-29) to a dully CL (Newberry 1-H-12) sparry calcite indicating a higher Fe/Mn ratio. Later, a moderately CL sparry calcite and a moderately CL microspar precipitated from a fluid with a moderate Fe/Mn ratio. Because of the small amount of pyrite observed in the calcite fracture fill, with more pyrite observed in the lower portion of the core and decreasing towards the upper portion, pyritization is assumed to have occurred relatively late in the paragenesis. Cross cutting relationships observed in the CL images indicate that late in the sequence a dully CL microspar precipitated from a fluid with higher Fe/Mn.

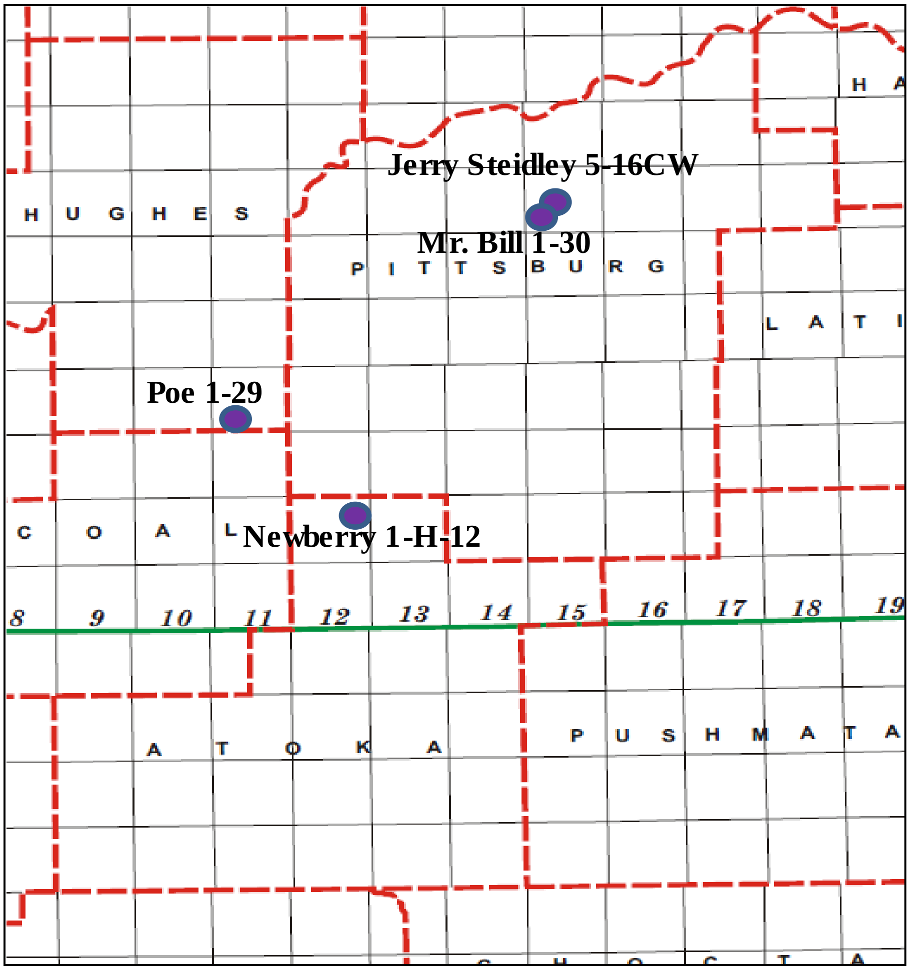

Fig. 4. Locations of the cores used in this study: Poe 1-29 in Hughes County, the Jerry Steidley 5-16 and Mr. Bill 1-30 in Pittsburg County, and the 1-H-12 Newberry well in Atoka County.

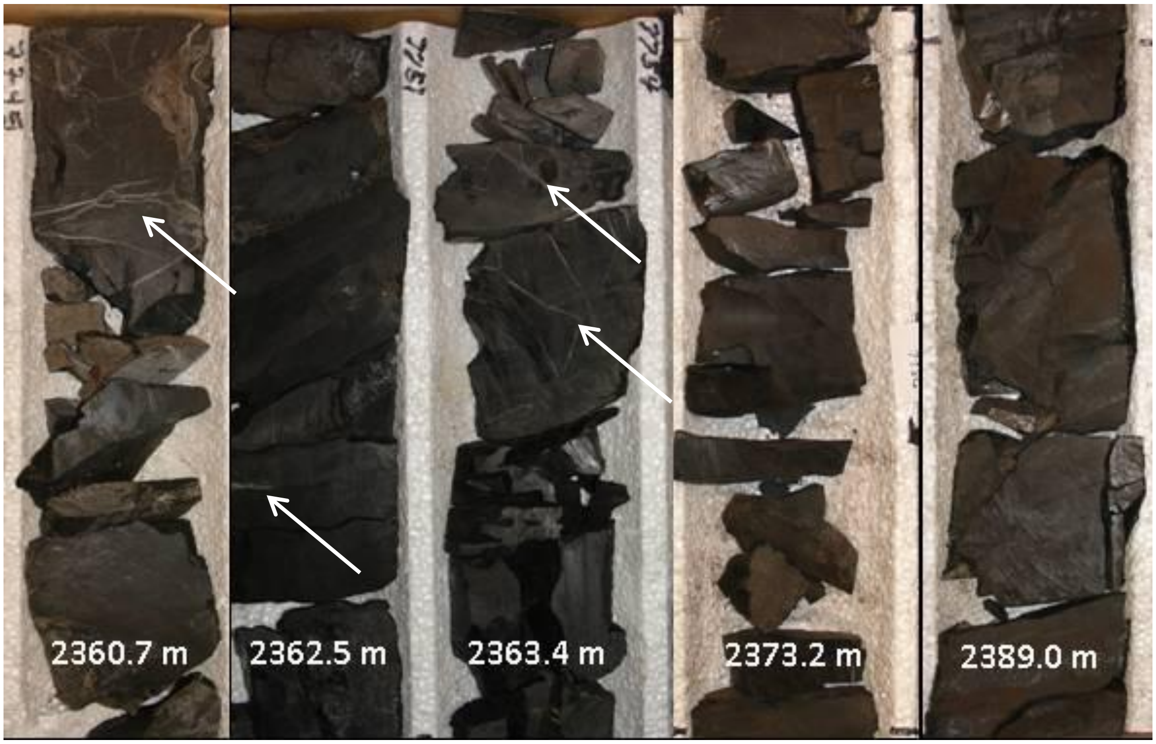

Fig. 5. Photographs of the Poe 1-29 core; the Woodford Shale is a black, silica rich, organic rich shale which contains horizontal and vertical fractures. The shale contains pyrite visible in hand sample.

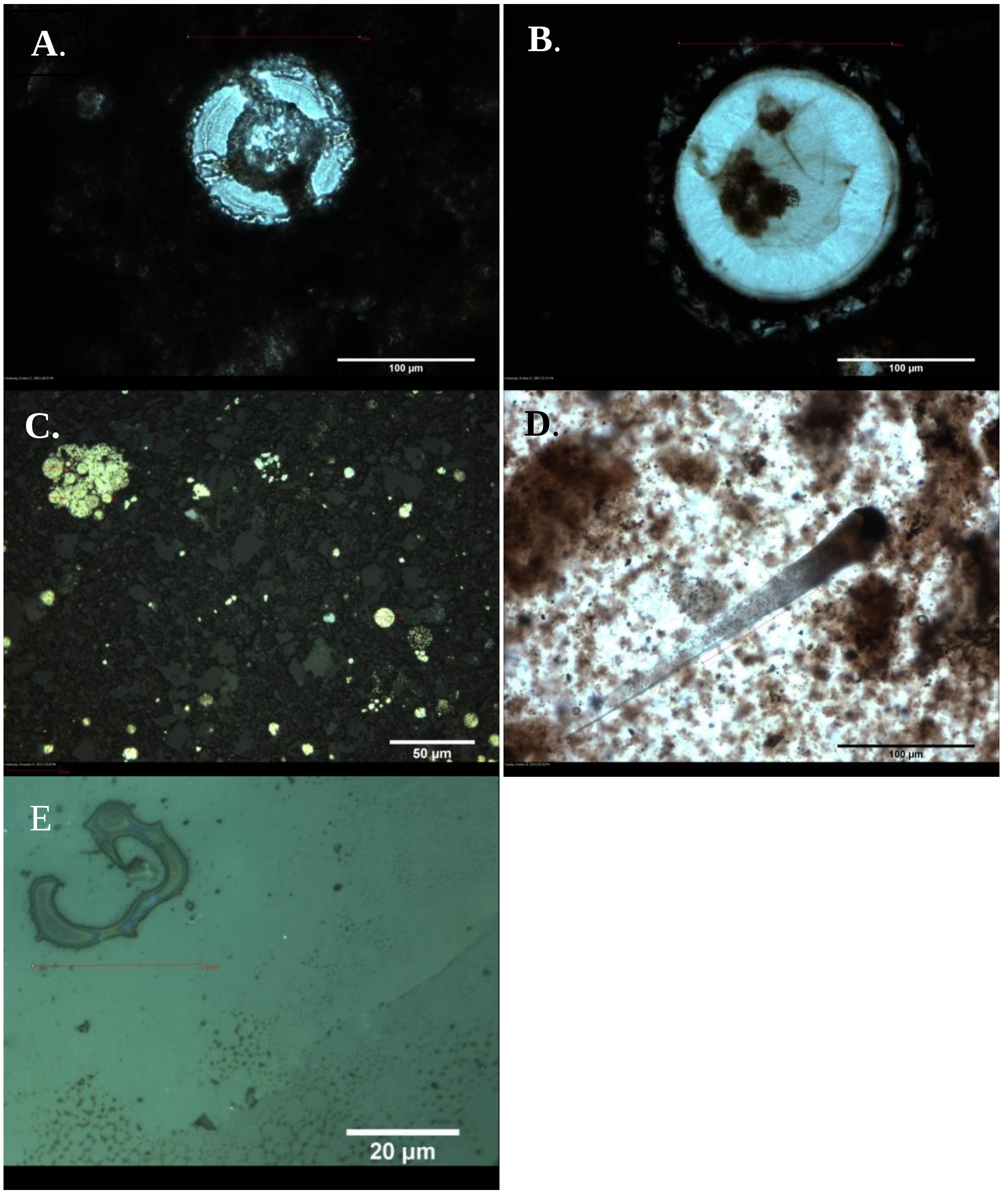

Fig. 6. Epi-fluorsecence images of constituents from various depths. A) Spumellarian radiolarian from depth 3995.3 m in the 1H-12 Newberry; B) Spumellarian Radiolarian from depth 2389.0 m in the Poe 1-29; C) Radiolarians in matrix at depth 2389.0 m in the Poe 1-29; D) Sponge spicule from depth 2360.4 m in the Poe 1-29; E) A shell fragment from depth 2384.8 m.

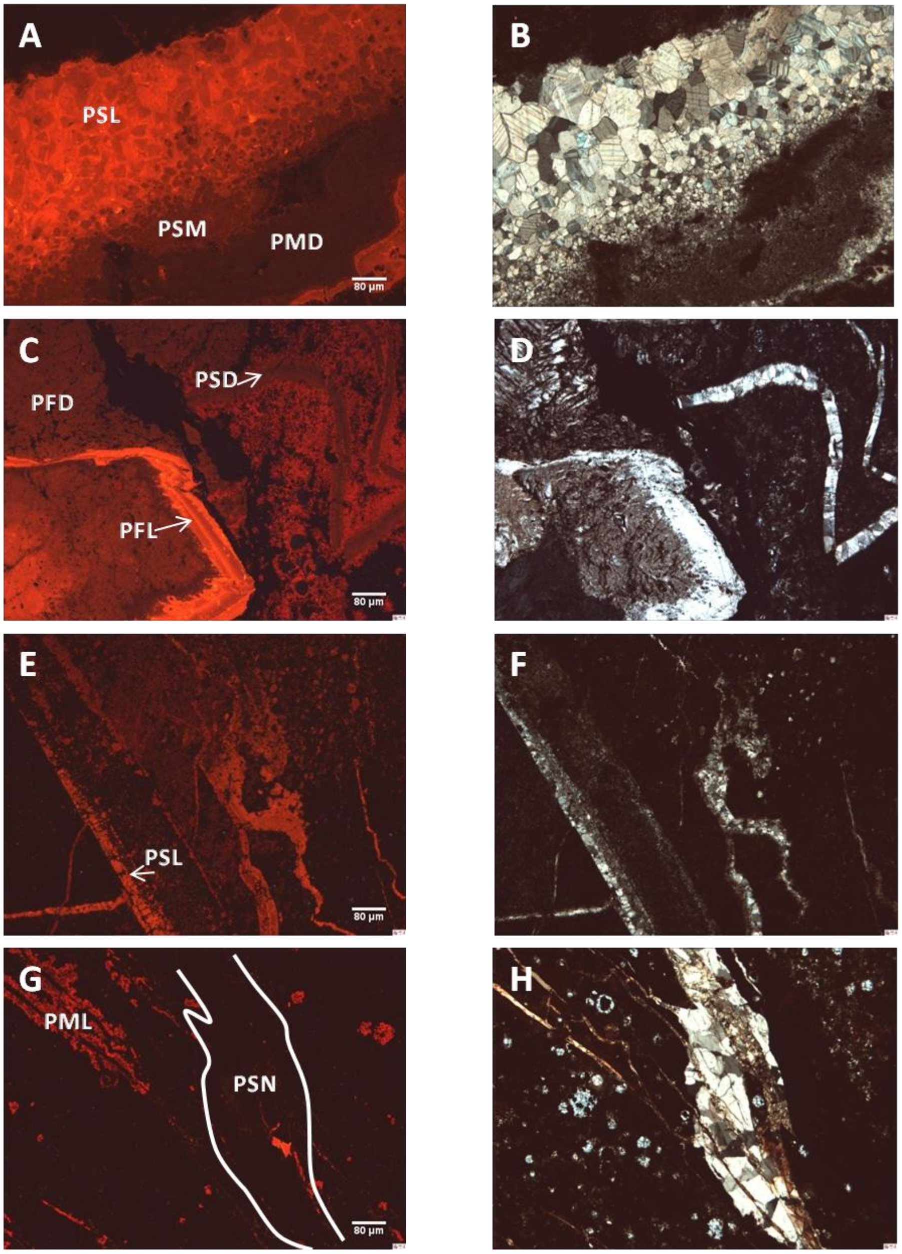

Fig. 7. A) and B) CL and plane polarized light (PPL) photographs showing calcite fracture fill at depth 2360.4 m in the Poe 1-29 core. PSL: CL sparry calcite, PSM: Moderately CL sparry calcite, PMD: dully CL micrite. Scale = 80 µm. C) and D) CL and PPL of brecciated zone in Poe 1-29 core, depth 2360.7 m. PSD: fracture with dully CL sparry calcite, PFD: dully CL fibrous calcite, PFL: CL zoned rim of fibrous calcite. Scale = 80 µm. E) and F) CL and PPL of fracture fill at depth 2362.5 m. PSL: CL sparry calcite fracture fill. Scale = 80 µm. G) and H) CL and PPL of depth 2389.0 m. PML: CL micrite in pore space of shale matrix, PSN: non-CL sparry calcite fracture fill. Scale = 80 µm.

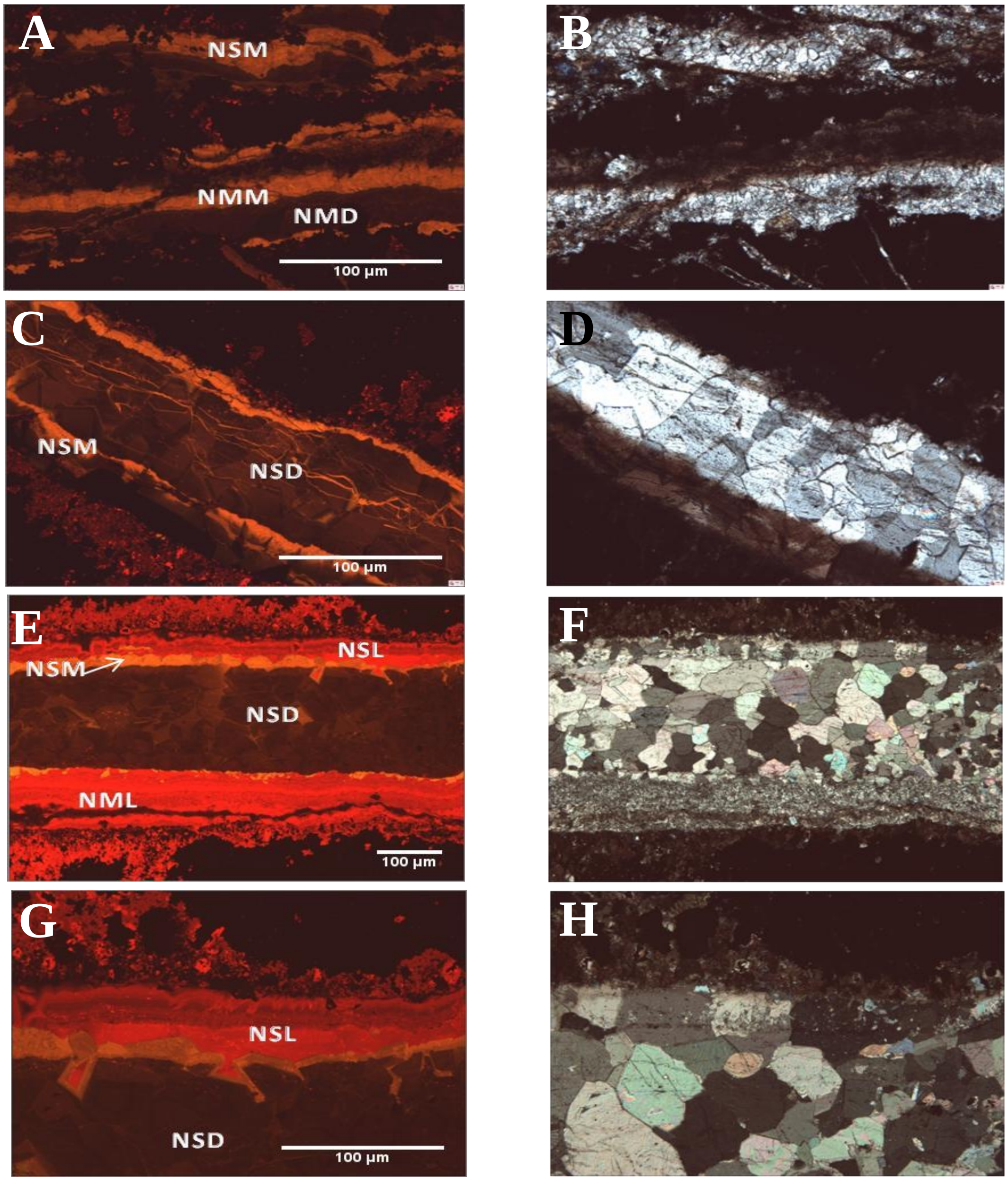

Fig. 8. A) and B) CL and PPL photomicrographs of calcite fracture fill in the Newberry 1-H-12 at a depth of 3995.3 m. NSM: moderately CL sparry calcite. NMM: moderately CL micrite. NMD: dully CL micrite. Scale bar = 100 µm. C) and D) CL and PPL of calcite fracture fill at same depth. NSM: moderately CL sparry calcite. NSD: dully CL sparry calcite. Scale bar = 100 µm. E) and F) CL and PPL of calcite fracture fill at depth of 3996.0 m. NSM: a yellowish, moderately CL sparry calcite. NSL: CL sparry calcite that transitions to CL micrite towards the fracture wall. NML: CL micrite. NSD: dully CL sparry calcite. Scale bar = 100 µm. G) and H) a magnification of the upper right of images E and F.

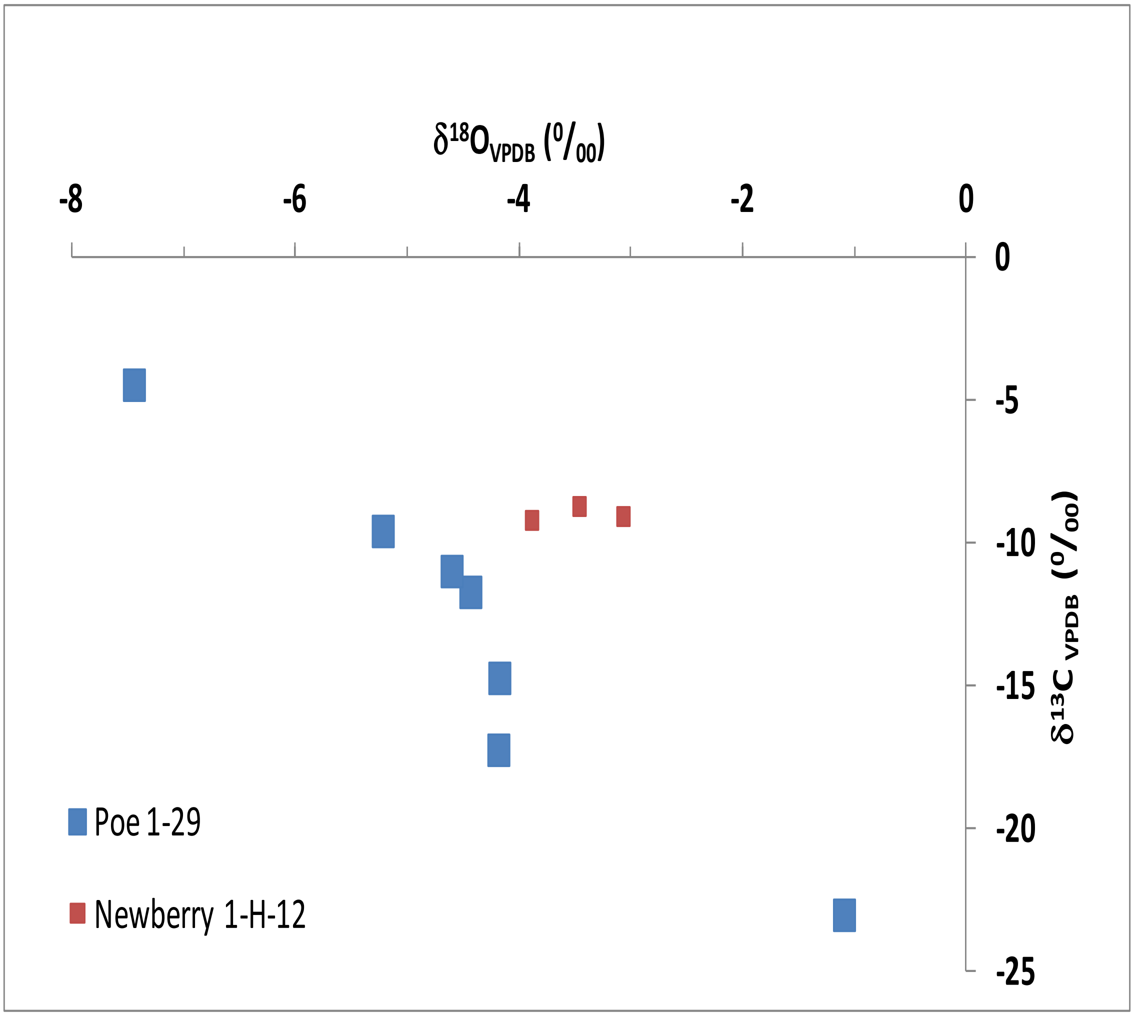

Fig. 9. Stable Carbon and Oxygen isotope data from the calcite fracture fill in the Poe 1-29 and the Newberry 1-H-12 cores.

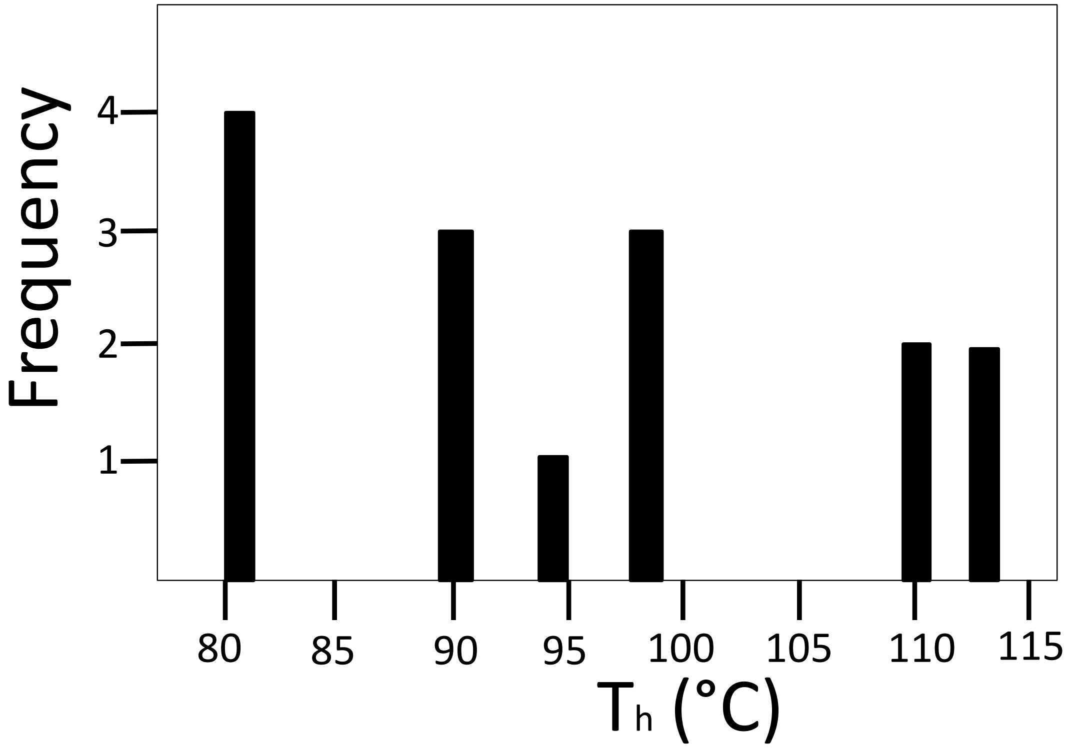

Fig. 10. Frequency of fluid inclusion homogenization temperatures for all samples from the Poe 1-29 and the Newberry 1-H-12.

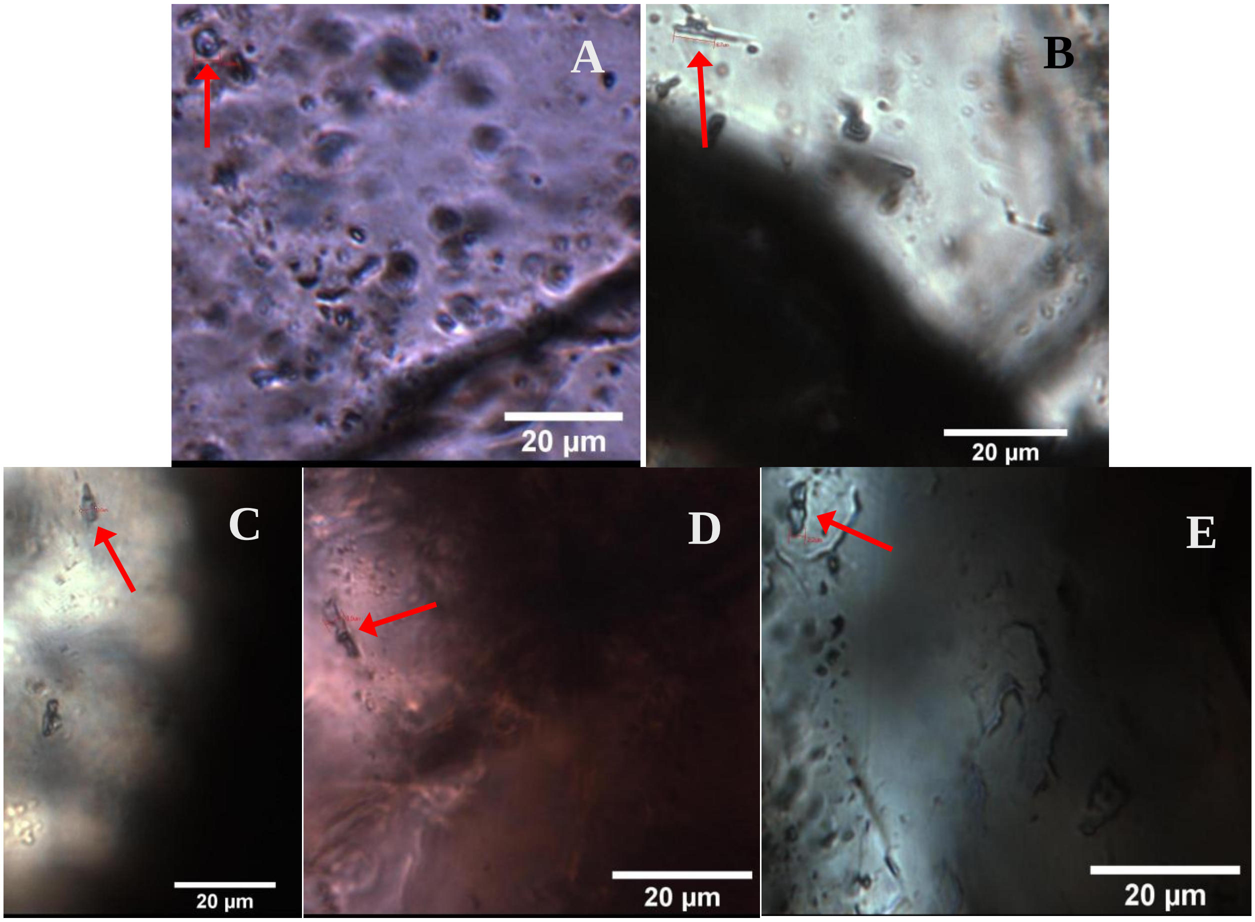

Fig. 11. Measured two phase fluid inclusions from the Poe 1-29 core. A) depth 2360.7 m secondary inclusion from CL zone PFD (Fig. 7C); B) depth 2360.7 m primary inclusion from CL zone PFL (Fig. 7C); C) depth 2373.2 m primary inclusion from CL zone PSL (Fig. 7A & E); D) depth 2373.2 m primary inclusion from CL zone PSL (Fig. 7A & E); E) depth 2373.2 m primary inclusion from CL zone PSL (Fig. 7A & E).

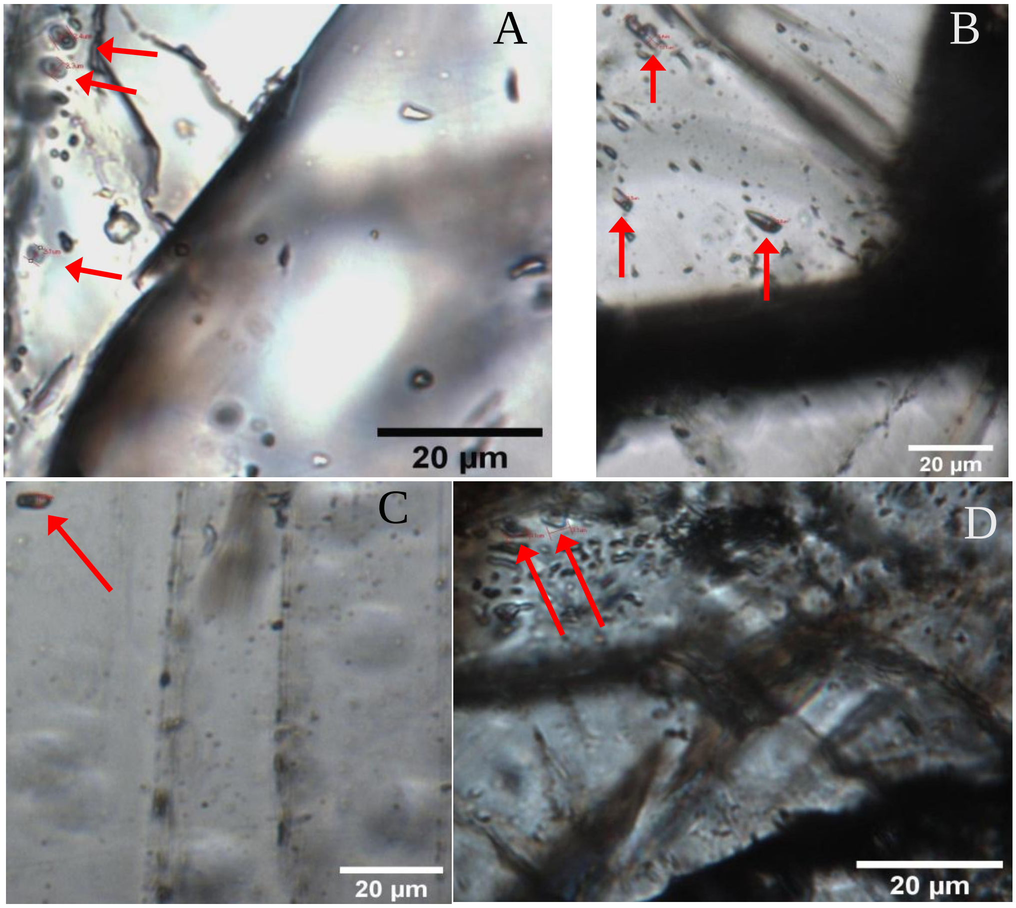

Fig. 12. Measured two phase fluid inclusion images from the Newberry 1-H-12. A) depth 3995.3 m primary fluid inclusion assemblage from CL zone of non-CL sparry calcite; B) depth 3995.6 m primary FI assemblage from CL zone NSD (Fig. 8E & G); C) depth 3995.6 m secondary inclusion from CL zone NSD (Fig. 8E & G); D) depth 3995.9 secondary FI assemblage from CLzone NSD (Fig. 8E & G).

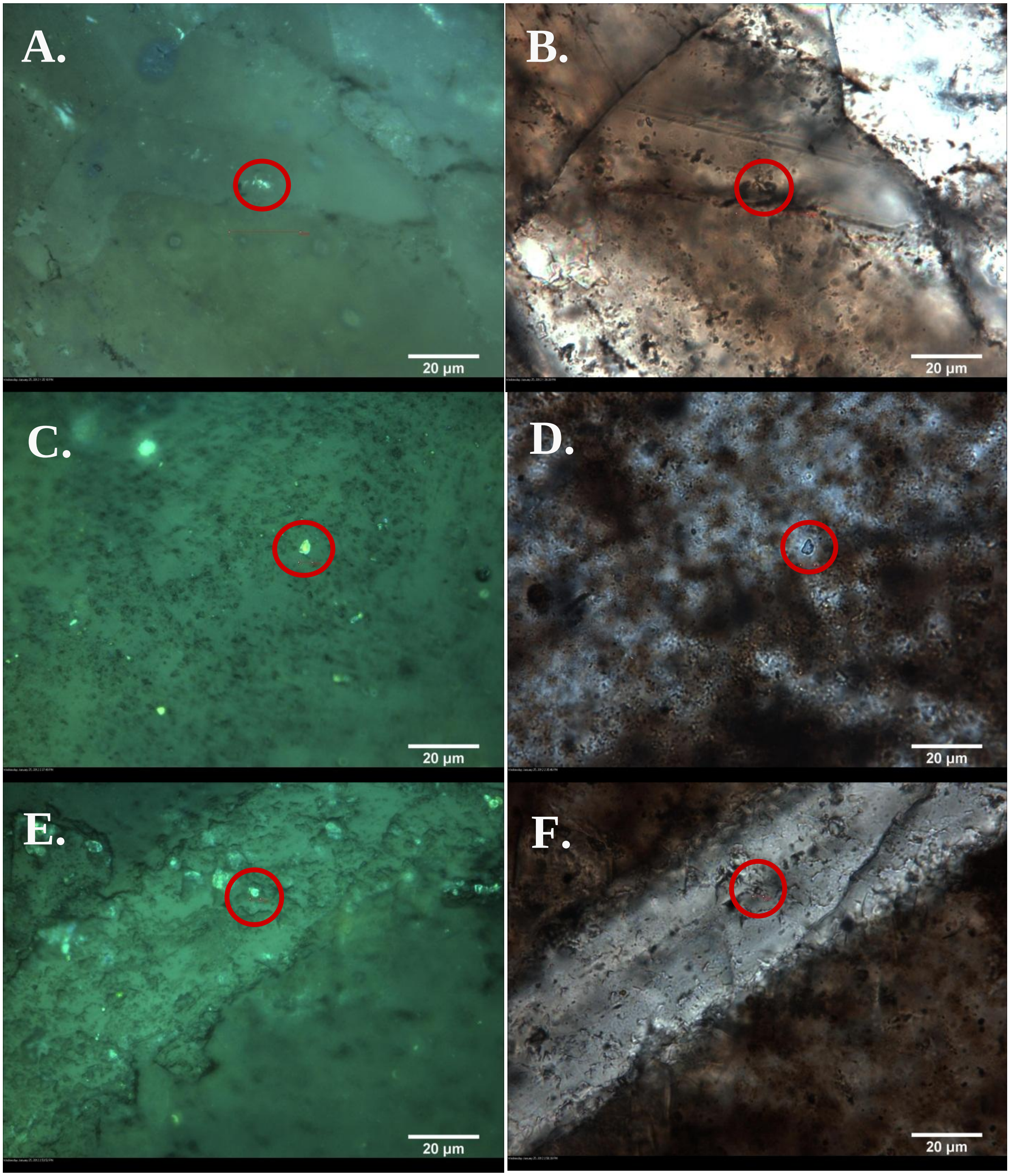

Fig. 13. Newberry 1-H-12 Core: A) Epi-fluorescence photomicrograph showing a one phase petroleum inclusion at depth 3995.3 m; B) A PPL image at the same depth. Poe 1-29 Core: C) FL image of one phase petroleum inclusion at depth 2360.4 m; D) A PPL image at the same depth; E) At depth 2360.4 m, a FL image of a one phase petroleum inclusion in a healed micro-fracture; F) PPL same image. Scale Bars = 20 µm. All inclusions fluoresced a pale yellow color indicating 25-30° API gravity.

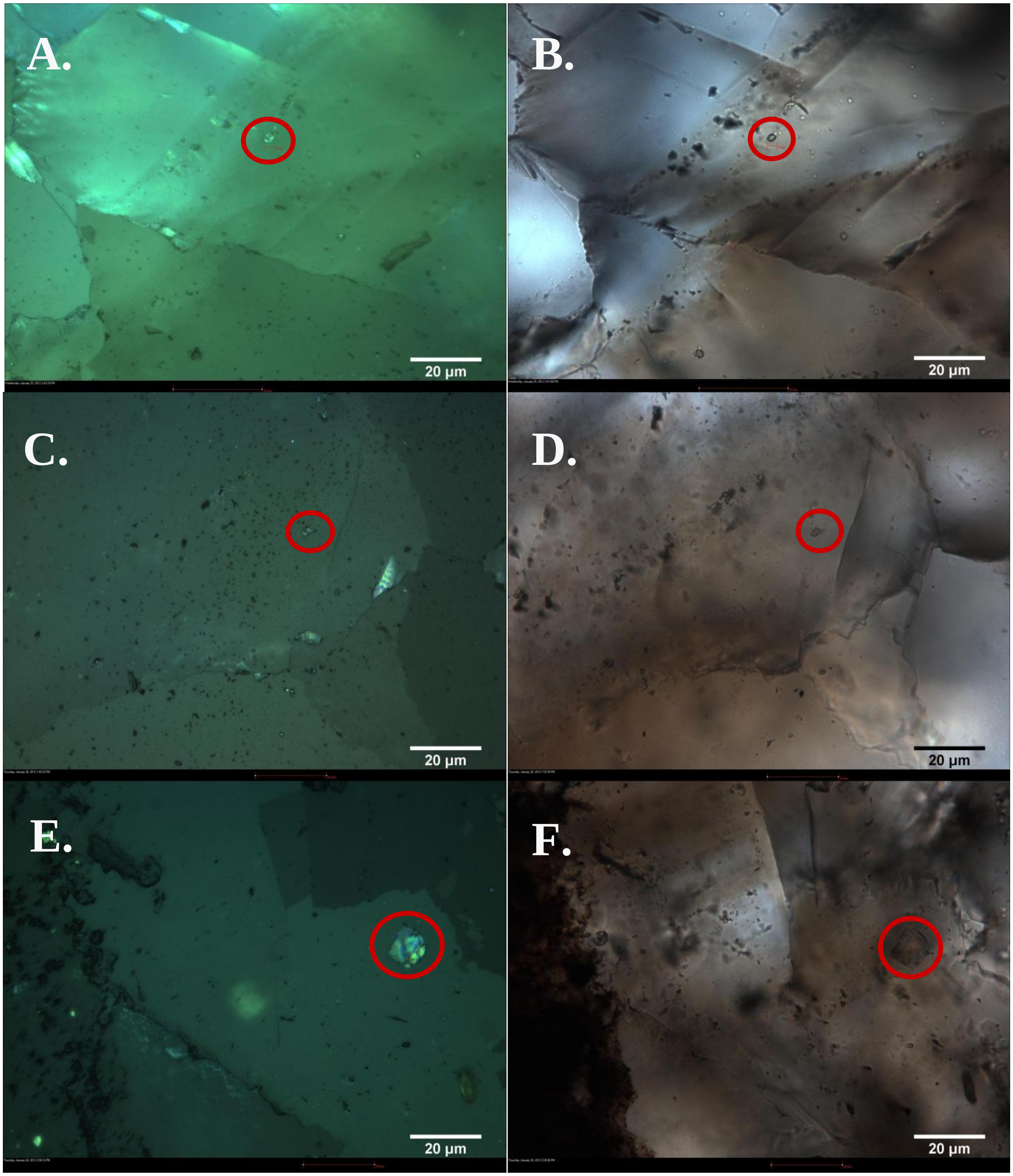

Fig. 14. FL images from the Poe 1-29. All images show one phase petroleum inclusions. A) Depth 2373.2 m, fluorescing pale yellow; B) Same image in PPL; C) Depth 2384.8 m fluorescing pale yellow; D) Same image in PPL; E) Large inclusion at depth 2384.8 m fluorescing a blue-green color, indicating 35-45° API; F) Same image in PPL. All scale bars= 20μm.

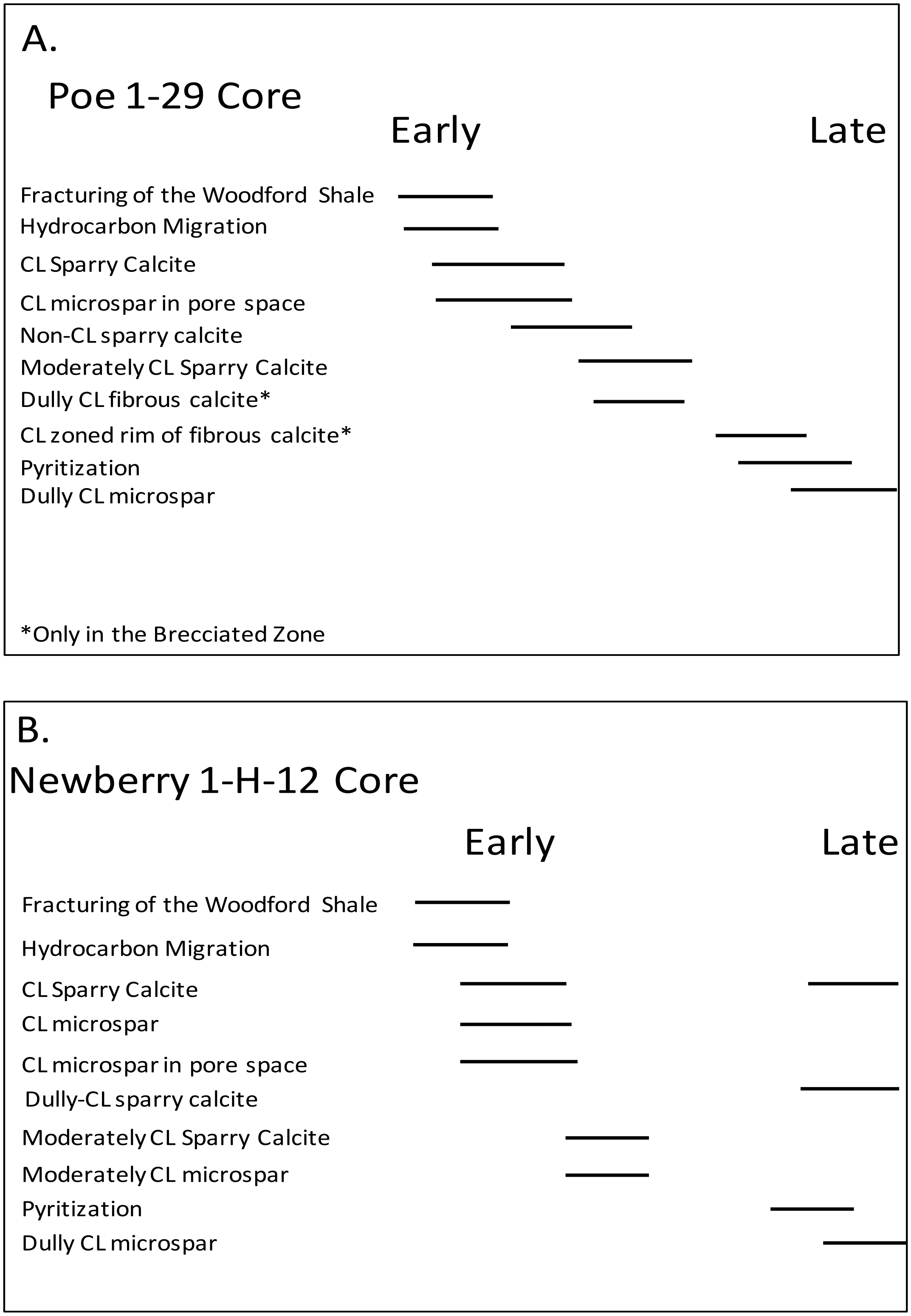

Fig. 15. Paragenetic sequences for the Poe 1-29 and the Newberry 1-H-12 cores displaying the timing of calcite precipitation.

CHAPTER V

Discussion

Shale Fracturing

The natural fractures observed in the Woodford Shale likely are the result of the brittleness of the silca rich shale (30-87% quartz; Cardott, 2008) subjected to tectonic stresses during the development of the Arkoma Basin. The Poe 1-29 and the Newberry 1-H-12 wells are located very near and north-west of the Frontal Thrust Belt of the Ouachita Mountains and the Choctaw fault. The Central Ouachitas lie to the southeast of the Frontal Thrust Belt and developed thrust-cored anticlines during the Mississippian (Hardie, 1990). Because the deposition of the Woodford Shale ended in the Early Mississippian (Tournaisian), and was faulted and folded by early Pennsylvanian time (Ataman, 2008), the initial movement and fracturing of the Woodford Shale must have occurred relatively early during diagenesis, approximately 20 million years after deposition.

Calcite Formation in Fractures

The source of the carbonate for the precipitation of the calcite fracture fill likely is derived from the underlying Hunton Limestone. The Mr. Bill 1-30 and the Jerry Steidley 5-16 CW wells are located in northern Pittsburg County (Fig. 4). In that location, the Hunton Group rocks are missing (Blackford, 2007), and the Woodford Shale is deposited on the Sylvan shale. Both the cores in that location lacked any fracture filling calcite and open horizontal and vertical fractures are observed. The Poe 1-29 and Newberry 1-H-12 contain fracture filling calcite and are located in areas where the Woodford Shale overlies Hunton Group carbonates indicating that the Hunton may have served as a source of carbonate for the precipitation of the calcite fracture fill. It should be noted, however that the calcite fracture fill could have been sourced locally during dewatering of the shale (see discussion below).

The fractures of the Poe 1-29 and the Newberry 1-H-12 contain calcites with varying CL zoning patterns (Fig. 7 & 8) indicating precipitation by fluids that varied in chemical composition. It is hypothesized that these fluids were derived during compaction and dewatering of the Woodford Shale. The CL intensity displayed by a zone of calcite is controlled by the Fe/Mn ratio of a given calcite zone (Frank et al., 1982). The Fe^{+2} and Mn^{2+} in the calcite are likely sourced from the dewatering of the Woodford Shale. During shale dewatering and compaction conversion of smectite and smectite/illite mixed layer clays to illite is a well-documented diagenetic process producing a large volume of free ions in solution (McHargue and Price, 1982). Silica and calcium released by the illititzation of smectite is transferred from shales to produce quartz overgrowths and calcite cements at temperatures as low as 60° C and Fe and Mg is released at temperatures >100° C (Boles and Franks, 1979). This temperature range is consistent with the homogenization temperatures of the measured fluid inclusions and within the oil window. This is a relatively early diagenetic process that occurs prior to the lithification of the sediment and with deeper burial, the conversion of smectite and mixed-layer illite/smectite to illite can produce significant quantities of Ca^{+2}, Mn^{+2} and Mg^{+2} (Boles and Franks, 1979).

Temperature of Calcite Formation

When a fluid inclusion assemblage yields consistent T_h data among inclusions of various sizes and shapes, the T_h of the inclusions are a measure of the minimum temperature at which they were entrapped, because no pressure corrections were applied to the T_h values (Reynolds and Goldstein, 1988). The average T_h values of the fluid inclusion assemblages observed in this study indicate that the minimum entrapment temperatures of the fluids range from 81.8-110° C. All inclusions had T_h values (Figure 15) that were consistent with the indicated geothermal gradient for the Arkoma Basin, which is 23°C/km (Lee et al., 1996).

One-phase petroleum inclusions observed in the calcite fracture fill (Fig. 13 &14) indicate that timing of the calcite formation is concurrent with hydrocarbon migration and are locally sourced from the Woodford Formation. High concentrations of Type II organic matter predispose the Woodford Shale to generate a large amount of oil during thermal maturation, plus, the Woodford would have reached effective oil saturation very rapidly with the initiation of thermal generation; causing oil expulsion to occur relatively early (Comer and Hinch, 1987). Thermal maturation of the Woodford Shale increases from west to east and with increasing present depth in the Arkoma Basin (Cardott, 2001). The one-phase petroleum inclusions observed in the fracture filling calcite cement indicate that concurrent with the hydrocarbon migration, calcite was precipitating in the fractures. The color of the fluorescence of these petroleum inclusions indicate oil with

25-35° API, which agrees well with previous findings of the Woodford mean API gravity of 39.9± 9.3° (Comer and Hinch, 1987). The contemporaneous timing of the calcite fracture fill and hydrocarbon expulsion is consistent with the hypothesis that the calcite fracture fill precipitated from fluid expelled from the dewatering shale and the smectite to illite transformation and is reflected by the paragenetic sequences (Fig. 15) for the Poe and Newberry cores. The homogenization temperatures, 81-110°C, are within the oil window, which ranges from 60-120°C (Selley, 1985).

Isotope Geochemistry

The $\delta^{18}O_{calcite}$ values support the hypothesis that the timing of the fracturing of the Woodford Shale and the calcite fracture fill precipitation occurred ~ 20 million years after deposition. The $\delta^{18}O_{calcite}$ values ranging from -1.1 to -7.4‰ VPDB plot well with Lower Carboniferous (Visean) sea-water (Popp et al., 1986). The wide ranges in the salinity values (Table 2, Appendix) indicate that fluids with fluctuating sodium chloride content, likely precipitated the calcite cements. This observation is consistent with an episodic release of ions during clay diagenesis. Timing and volume of fluid flow depend on compaction of the shale and expulsion of structural water carrying ions released during clay diagenesis. The rate of diffusion depends on several variables such as: temperature, nucleation sites, distances of diffusion and porosity (McHargue and Price, 1982). These variables allow for a wide range of salinity values. This observation is further supported by the CL calcite zonation that was observed. The average salinity value for the Newberry core is 8.10 wt% NaCl and found at a depths of ~3995 m. The average salinity value of the Poe core is 4.07 wt% NaCl and found at depths of ~ 2360 m. The Newberry values are from much greater depths and are much higher salinity. This observation is consistent with the clay diagenesis hypothesis for the origin of the precipitating fluids. With increasing burial and depth, clay diagenesis increases, increasing available fluid and free ions.

The $\delta^{13}C$ isotope values (Table 1, Appendix) are consistent calcite precipitation in the zone of thermochemical sulfate reduction (TSR) during burial diagenesis. The wide range of $\delta^{13}C$ values of -4.4 to -23‰ VPDB over a smaller range of $\delta^{18}O_{calcite}$ values from -1.05 to -7.40‰ VPDB indicates the incorporation of variable amounts of isotopically light carbon derived from the oxidation of organic carbon at temperatures above 60°C (Machel et al., 2000). An example of similar trends are observed in the carbon isotopic composition of host calcite in the Dagmar and Skjold fields in the Danish North Sea, which are as light as -16.5‰ VPDB. This was interpreted to indicate that biodegradation of the oils was the source of some of the carbon in the calcite and sulfate reduction was the source of sulfur for pyritization (Jensenius and Burruss, 1990). TSR is consistent with the extremely depleted $\delta^{13}C$ isotope values and the numerous pyrite lenses and bands observed in the Woodford cores.

CHAPTER VI

Conclusions

Based on the petrography, fluid inclusion analysis and stable isotope data of the calcite fracture fill in core samples of the Woodford Shale, the following conclusions are made. 1) Timing of the deposition of Woodford sediments and the deformation of the Arkoma basin during the Pennsylvanian, indicate that fracturing occurred within about 20 million years after deposition, relatively early after the initial deposition and compaction of the Woodford sediments. 2) The source of the carbonate for the precipitation of the calcite fracture fill likely is from the underlying Hunton Group rocks. 3) The fractures in the Poe 1-29 and the Newberry 1-H-12 contain calcites with varying CL zoning patterns indicating precipitation by fluids with fluctuating ionic content. The variation in fluid chemistry likely is the result of smectite and illite/smectite to illite transformation during compaction and dewatering of the Woodford Shale. 4) The minimum entrapment temperatures of the fracture filling calcite cements range from 81.8-110 ° C. This temperature range agrees well with the indicated geothermal gradient for the Arkoma Basin during the early Pennsylvanian. 5) One-phase petroleum inclusions, observed in the calcite fracture fill, indicate that the timing of calcite cement precipitation is concurrent with hydrocarbon generation. These hydrocarbons are locally sourced from the Woodford Shale. 6) The $\delta^{18}O_{calcite}$ values ranging from -1.1 to -7.4‰ VPDB are consistent with Lower Carboniferous (Visean) sea-water values. The wide range in salinity values that increase with depth supports the clay diagenesis hypothesis for the origin of the calcite precipitating fluids. 7) A wide range of depleted $\delta^{13}C$ values relative to a small range of depleted $\delta^{18}O_{calcite}$ values indicates incorporation of variable amounts of isotopically light carbon derived from the oxidation of organic carbon in the zone of thermochemical sulfate reduction.

REFERENCES

Amsden, T. W., 1967, Devonian of the southern mid-continent area, United States, in W. M. Caplan, P. L. Hilpman, E. H. McGlasson, T. L. Rowland, and O. A. Wise, Jr., eds., Canada, p. 913-932.

Amsden, T. W., 1972, Misener Sandstone (Middle-Upper Devonian), North-Central Oklahoma, in G. Klapper, ed., American Association of Petroleum Geologists Bulletin, United States, American Association of Petroleum Geologists : Tulsa, OK, United States, p. 2323-2334.

Amsden, T. W., 1975, Hunton Group (Late Ordovician, Silurian, and Early Devonian) in the Anadarko Basin of Oklahoma, *Bulletin - Oklahoma Geological Survey*: Norman, OK, United States, p. 121,214.

Amsden, T. W., 1980, Hunton Group (Late Ordovician, Silurian, and Early Devonian) in the Arkoma Basin of Oklahoma, *Bulletin - Oklahoma Geological Survey*, Norman, OK, United States, p. 129,136.

Barrick, J. E., 1990, Conodont fluorescence emission spectra; potential for high resolution evaluation of organic maturation in hydrocarbon-bearing basins, D. J. Over, C. R. Landis, and W. L. Borst, eds., Abstracts with Programs - Geological Society of America, United States, Geological Society of America (GSA) : Boulder, CO, United States, 22, p. 1-2.

Berryman, R. R., Blythe, J. W., Puckette, J.O, Catlos, E. J, 2007, Electron Microprobe Analysis of Fracture filling cements in the Woodford Shale, SE Oklahoma. GSA Meeting Abstracts: BTH 183, p.118-110.

Blackford, M.A., 2007, Electrostratigraphy, Thickness, and Petrophysical Evaluation of the Woodford Shale, Arkoma Basin, Oklahoma, Thesis: Oklahoma State University, p. 1-84, unpublished.

Brown, D., 2008, Operators flocking to the play; big potential boosts the Woodford, AAPG Explorer, United States, American Association of Petroleum Geologists : Tulsa, OK, United States, p. 12.

Bodnar, R. J,1992, Revised equation and table for freezing point depressions of H2O-salt fluid inclusions (Abstract): PACROFI IV, Fourth Biennial Pan-American

Conference on Research on Fluid Inclusions, Program and Abstracts, Lake Arrowhead, CA, v. 14, p. 15.

Cander, H., and T. L. Patton, 2007, Regional petroleum systems evaluation and new play identification in an uplifted Paleozoic basin; Arkoma Basin, Oklahoma, USA, in T. L. Patton, ed., Abstracts: Annual Meeting - AAPG, United States, AAPG and Society for Sedimentary Geology: Tulsa, OK, United States, p. 20.

Cardott, B. J., 2001, Thermal maturation of the Woodford Shale in eastern Oklahoma, Circular - Oklahoma Geological Survey, United States, University of Oklahoma: Norman, OK, United States, p. 193-193.

Cardott, B.J., 2008, Overview of Woodford gas-shale play of Oklahoma, U.S.A: Abstracts: Annual Meeting - American Association of Petroleum Geologists, v. 2008.

Cemen, I., A. Zuhair, et al. (1996), Geometry of Thrusting in the Wilburton Gas Field and Surrounding Areas, Arkoma Basin, Oklahoma; Implications for Gas Exploration in the Spiro Sandstone Reservoirs, Tulsa Geological Society, p. 84.

Comer, J. B., and H. H. Hinch, 1987, Recognizing and quantifying expulsion of oil from the Woodford Formation and age-equivalent rocks in Oklahoma and Arkansas: AAPG Bulletin-American Association of Petroleum Geologists, v. 71, p. 844-858.

Comer, J. B., 1991, Report of Investigations - Texas, University, Bureau of Economic Geology Stratigraphic analysis of the Upper Devonian Woodford Formation, Permian Basin, West Texas and southeastern New Mexico, Report of Investigations - Texas, University, Bureau of Economic Geology, United States, University of Texas at Austin, Bureau of Economic Geology : Austin, TX, United States, p.1-63.

Comer, J. B., 1992, Potential for producing oil and gas from the Woodford Shale (Devonian-Mississippian) in the southern Mid-Continent, USA, Transactions - Southwest Section A.A.P.G., United States, American Association of Petroleum Geologists : [location varies], United States, p. 290-290.

Comer, J. B., 1992b, Organic geochemistry and paleogeography of Upper Devonian formations in Oklahoma and northwestern Arkansas, Circular - Oklahoma

Geological Survey, United States, University of Oklahoma : Norman, OK, United States, p. 70-93.

Comer, J. B., 2005, Facies distribution and hydrocarbon production potential of Woodford Shale in the southern Midcontinent, Circular - Oklahoma Geological Survey, United States, University of Oklahoma: Norman, OK, United States, p. 51-62.

Coplen, T.B., Kendall C, Hopple J, 1983, Comparison of stable isotope reference samples, Nature, 302, p. 236-238.

Dickinson, W. R., 1974, Plate tectonics and sedimentation, Special Publication - Society of Economic Paleontologists and Mineralogists, United States, SEPM (Society for Sedimentary Geology) : Tulsa, OK, United States, p. 1-27.

Elmore, R. D., P. K. Sutherland, et al. (1990). Middle Pennsylvanian Recurrent Uplift of the Ouachita Fold Belt and Basin Subsidence in the Arkoma Basin, Oklahoma, Geology, v. 18(9), p. 906-909.

Frank, J. R., A. B. Carpenter, et al. (1982). Cathodoluminescence and composition of calcite cement in the Taum Sauk Limestone (Upper Cambrian), Southeast Missouri, Journal of Sedimentary Petrology, v. 52(2), p. 631-638.

Hardie, W. E. (1990). Subsurface structural study of the buried Ouachita thrust front, southeastern Oklahoma, Shale Shaker, v. 41(2): 32-55.

Hass, W. H., 1965, Late Devonian and Early Mississippian age of the Woodford Shale in Oklahoma, as determined from conodonts, in J. W. Huddle, ed., U. S. Geological Survey Professional Paper, United States, U. S. Geological Survey : Reston, VA, United States, p. D125-d132.

Jensenius, J. and Burruss, R. C. (1990). Hydrocarbon-water interactions during brine migration; evidence from hydrocarbon inclusions in calcite cements from Danish North Sea oil fields, Geochimica et Cosmochimica Acta, v. 54(3),p. 705-713.

Lambert, M. W., 1991, Internal Stratigraphy and Organic Facies of the Devonian-Mississippian Chattanooga Shale in Kansas and Oklahoma: AAPG Bulletin-American Association of Petroleum Geologists, v. 75, p. 616-617.

Lambert, M. W., 1994, Revised Upper Devonian and Lower Mississippian stratigraphic nomenclature in Kansas, Bulletin - Kansas Geological Survey, United States, Kansas Geological Survey : Lawrence, KS, United States, p. 74-78.

Lee, Y. M., D. Deming, et al., 1996, Heat flow and heat production in the Arkoma Basin and Oklahoma Platform, southeastern Oklahoma." Journal of Geophysical Research-Solid Earth, v. 101(B11): 25387-25401.

Machel, H.G., Cavell, P.A., Patey, K.S., 1996, Isotopic Evidence for Carbonate Cementation and recrystallization, and for tectonic expulsion of fluids into the Western Canada Sedimentary Basin, GSA Bulletin, v. 108**,** n. 9, 1108-1119.

Machel, H. G., Cavell, P. A., et al., 2000, Tectonically induced fluid flow in Devonian carbonate aquifers of the Western Canada Sedimentary Basin, Journal of Geochemical Exploration, v. 69-70, p. 213-217.

Popp, B. N., T. F. Anderson, et al., 1986, Brachiopods as indicators of original isotopic compositions in some Paleozoic Limestones, Geological Society of America Bulletin, v. 97(10), p. 1262-1269.

Reynolds, J.T. and Goldstein, R. H., Systematics of Fluid Inclusions in Diagenetic Minerals, SEPM Short Course 31, p. 1-213.

Selley, R.C., 1985, Generation and Migration of Petroleum, *in “*Elements of Petroleum Geology”, Academic Press, p. 181-237.

Sutherland, P. K., 1988, Late Mississippian and Pennsylvanian depositional history in the Arkoma Basin area, Oklahoma and Arkansas. United States, Geological Society of America (GSA): Boulder, CO, United States, v. 100, p. 1787-1802.

Thomas, W. A., and Viele, G. W., 1983, Tectonic History of the Ouachita Orogen: Geology, v. 11, p. 482-483.

Thomas, W. A., 2004, Genetic relationship of rift-stage crustal structure, terrain accretion, and foreland tectonics along the southern Appalachian-Ouachita Orogen, Journal of Geodynamics, v. 37, p. 549-563.

APPENDIX

Table 1.

Sample id	Sample id	meters	$\delta^{13}C$ VPDB(‰)	$\delta^{18}O_{calcite}$ VSMOW (‰)	$\delta^{18}O_{calcite}$ VPDB (‰)
N13108	N13109	3995.3	-8.691	27.293	-3.464
N13109	N13110	3995.6	-9.178	26.855	-3.889
N13110	N13111	3995.9	-9.044	27.698	-3.071
P7744	P7745	2360.4	-23.026	29.779	-1.053
P7745	P7746	2360.7	-14.718	26.600	-4.136
P7751	P7752	2362.5	-17.239	26.591	-4.145
P7786	P7787	2373.2	-11.703	26.333	-4.395
P7824	P7825	2384.8	-9.567	25.525	-5.179
P7838	P7839	2389.0	-10.973	26.160	-4.563
P7796	P7797	2376.2	-4.438	23.230	-7.406
P7824*	P7824*	2384.8	-10.380	25.747	-4.964
P7770*	P7770*	2368.3	-10.900	26.499	-4.234
* These Measurements were taken eas were taken earlier in the study.					

$$\delta^{18}O_{calcite}\ (VPDB)=\delta^{18}O_{calcite}\ (VSMOW)*0.97002-29.98$$

(Coplen et al., 1983)

Table 2.

Core	Sample id.	T_h (°C)	T_{fm} (°C)	T_m (°C)	wt% NaCl**	FI Type	CL Zone	Phases
Poe 1-29	7745…8 4b	X	-19.5	-2.7	4.49	S	Dully CL Fiberous	1 No FL*
Poe 1-29	7745__100X_S1	94.4	-17.9	-1.2	2.07	P	CL Fiberous	2 No FL
Poe 1-29	7786_100x_1	80	-32.9	-0.1	0.18	P	CL Sparry	2 No FL
Poe 1-29	7786_100x_3	113	-29.8	-4.5	7.17	P	CL Sparry	2 No FL
Poe 1-29	7786_100X_4	113	-35	-4.0	6.45	P	CL Sparry	2 No FL
1H-12 Newberry	13108 FIA=3	90.2	-31.4	8.3	12.05	P	Non-CL Sparry	2 No FL
1H-12 Newberry	13109 1B FIA=3	81.8	-33	3.9	6.30	P	Dully CL Sparry	2 No FL
1H-12 Newberry	13109 3A	97.3	-37.7	7.8	11.46	S	Dully CL Sparry	2 No FL
1H-12 Newberry	13110_100X_1 FIA=2	110	-21.4	-1.5	2.57	S	Dully CL Sparry	2 No FL
*nucleated after heating								
** Calculated after Bodnar (1992)								

T_h (°C)	The Homogenization Temperatures
T_{fm} (°C)	The First Melting Temperatures
T_m (°C)	The Final Melting Temperatures
wt% NaCl**	The weight percent of Sodium Chloride
FI Type	Type of Fluid Inclusion measured
CL Zone	Zone of Cathodoluminescence Intensity the inclusion was observed
Phases	The number of phases within the inclusion
FL	Excitation observed under epi-fluorescence

Table 3.

Core	Avg. T_h (°C)	Avg. $\delta^{18}O_{calcite}$ (VSMOW ‰)	Calculated $\delta^{18}O_{water}$ (VSMOW ‰)
Poe 1-29	100.1	26.3	26.0
Newberry 1-H-12	94.8	27.3	26.7

Avg. T_h (°C) = The Average Homogenization Temperature in degrees Celsius.
Avg. $\delta^{18}O_{calcite}$ VSMOW (‰) = Average delta value for calcite vs. the VSMOW (Vienna Standard Mean Ocean Water) in per mill.
Avg. $\delta^{18}O_{water}$ VSMOW (‰) = Average delta value for the formation waters vs. the VSMOW standard in per mill.

Table 4. Diagram showing the sequence of diagenetic events for the calcite fracture fill.

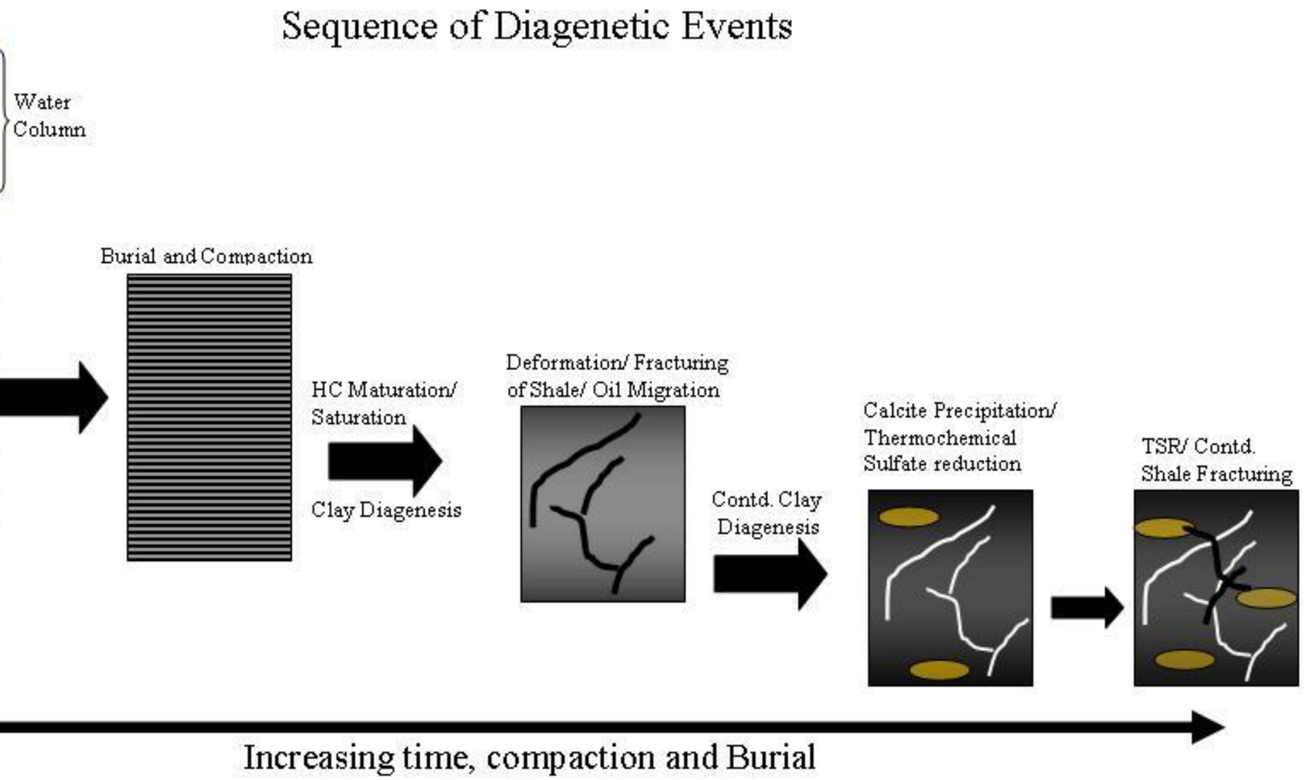

VITA

Jacqueline Rene Berryman

Candidate for the Degree of

Master of Science

Thesis: TIMING AND PARAGENESIS OF THE CALCITE FRACTURE FILL IN THE WOODFORD SHALE

Major Field: Petroleum Geology

Biographical:

Education:
Completed the requirements for the Master of Science in Geology at Oklahoma State University, Stillwater, Oklahoma in July, 2012

Experience:
EOG Resources Summer Internship, May 2009- August 2009
3817 NW Expressway, Oklahoma City, OK 73112-1489

Teaching Assistant, August 2007 to May 2009
Oklahoma State University, Boone Pickens School of Geology, Stillwater Campus

Professional Memberships: American Association of Petroleum Geologist, Geological Society of America. Oklahoma City Geological Society, Tulsa Geological Society.

Name: Jacqueline Rene Berryman Date of Degree: July, 2012

Institution: Oklahoma State University Location: Stillwater, Oklahoma

Title of Study: TIMING AND PARAGENESIS OF THE CALCITE FRACTURE FILL IN THE WOODFORD SHALE

Pages in Study: 44 Candidate for the Degree of Master of Science

Major Field: Petroleum Geology

Scope and Method of Study:

This study characterizes the precipitating fluid of calcite fracture fill in core samples of the Woodford Shale. A geochemical and petrographical study was performed using fluid inclusion microthermometry, cathodoluminescence petrography, epi-fluorescence imaging and stable carbon and oxygen isotope geochemistry.

Findings and Conclusions:

The Woodford Shale in the Arkoma Basin of Oklahoma is brittle and highly fractured. In some areas of the basin these fractures are cemented with calcite cement. This study uses petrography, fluid inclusion analysis, and carbon and oxygen stable isotope geochemistry to analyze the calcite fracture fill obtained from core samples to characterize the precipitating fluid and to develop a paragenetic sequence for the diagenetic events occurring within the shale that led to the precipitation of the calcite fracture fill.

Because of the timing of the formation of the Woodford shale and the deformation of the Arkoma basin in the Pennsylvanian time, initial movement and fracturing of the Woodford shale must have occurred between 326-345 ma., relatively early after the formation and compaction of the Woodford shale. Where the Woodford shale overlies the Hunton Group rocks, the fractures are likely to contain calcite fracture fill because the Hunton serves as a source of carbonate, facilitating the precipitation of calcite. The precipitating fluid had minimum entrapment temperatures that range from 81.8-110° C and are consistent with the indicated geothermal gradient of the Arkoma Basin. One phase petroleum inclusions found in the calcite fracture fill indicate that hydrocarbons were migrating as the fractures were being cemented. The wide range of salinity values calculated from the microthermometry indicates a multiple fluid history and is supported by the zonation of calcites observed using cathodoluminescence petrography. The wide range of depleted $\delta^{13}C$ over a smaller range of depleted $\delta^{18}O_{calcite}$ indicates the incorporation of variable amounts of isotopically light carbon derived from the oxidation of organic carbon, indicating diagenesis in the zone of thermochemical sulfate reduction.

ADVISER’S APPROVAL: Dr. Jay Mason Gregg